Bioelectrochemistry 108 (2016) 46–53

Contents lists available at ScienceDirect

Bioelectrochemistry

journal homepage: www.elsevier.com/locate/bioelechem

Modeling of laccase inhibition by formetanate pesticide using theoretical approaches☆

Ana C.V. Martins [a], Francisco W.P. Ribeiro [a], Geancarlo Zanatta [b], Valder N. Freire [c], Simone Morais [d], Pedro de Lima-Neto [a], Adriana N. Correia [a,*]

[a] Departamento de Química Analítica e Físico-Química, Centro de Ciências, Universidade Federal do Ceará, Bloco 940, Campus do Pici, 60440-900 Fortaleza, CE, Brazil
[b] Departamento de Bioquímica, Universidade Federal do Rio Grande do Sul, 90035-003 Porto Alegre, RS, Brazil
[c] Departamento de Física, Universidade Federal do Ceará, Caixa Postal 6030 Campus do Pici, 60455-760 Fortaleza, CE, Brazil
[d] REQUIMTE, Instituto Superior de Engenharia do Porto, Rua Dr. António Bernardino de Almeida 431, 4200-072 Porto, Portugal

ARTICLE INFO

Article history:
Received 2 October 2015
Received in revised form 12 December 2015
Accepted 17 December 2015
Available online 21 December 2015

Keywords:
Enzymatic catalysis
Inhibition
Amino acid residues
Quantum chemical calculations
Density functional theory
Molecular docking

ABSTRACT

The inhibition of laccase enzymatic catalytic activity by formetanate hydrochloride (FMT) was investigated by cyclic voltammetry and by quantum chemical calculations based on density functional theory with a protein fragmentation approach. The cyclic voltammograms were obtained using a biosensor prepared by enzyme immobilization on gold electrodes modified with gold nanoparticles and 4-aminophenol as the target molecule. The decrease in the peak current in the presence of FMT was used to characterize the inhibition process. The calculations identified Asp206 as the most relevant moiety in the interaction of FMT with the laccase enzymatic ligand binding domain. The amino acid residue Cys453 was important, because the Cys453–FMT interaction energy was not affected by the dielectric constant, although it was not a very close residue. This study provides an overview of how FMT inhibits laccase catalytic activity.

1. Introduction

The contamination of water and food with pesticides has made the monitoring of this class of compounds a research topic of great interest in the 21st century [1,2]. Since the 1940s, the industrial production of such compounds has increased, and it continues to do so. Among several classes of pesticides, carbamate compounds are widely used insecticides and acaricides. Formetanate hydrochloride (3-dimethylaminomethyleneaminophenyl methylcarbamate hydrochloride, FMT) is applied to several agricultural crops, including grapes, mangoes, potatoes, onions, citrus fruits, beans, watermelons, peppers and tomatoes. Despite the success of FMT in pest control for the aforementioned agricultural crops, the chemical is on the priority list released by the United States Environmental Protection Agency (US EPA Regulating Pesticides) [3] because FMT is soluble in water and because the compound causes neurotoxicity due to inhibition of the enzyme acetylcholinesterase [4–7]. Therefore, analysis of the FMT residue in food and aquatic environments is an issue of great interest.

Enzymatic electrochemical biosensors are environmentally friendly, allow miniaturization and are inexpensive, and thus may be useful in the analytical detection of pesticides [8,9]. To analyze FMT and other carbamate pesticides in water and in fruits, various electrochemical biosensors have been proposed; these biosensors combine laccase enzyme (Lac) with several transductors such as composite paste electrodes with carbon ceramic [10], multi-walled carbon nanotubes [11], platinum nanoparticles-ionic liquid-graphite [12], Prussian blue film-grapheme [13], gold nanoparticle-chitosan-grapheme [14], and gold electrodes modified with gold nanoparticles (AuNPs) 15]. The rationale for these electrochemical biosensors is that carbamate compounds inhibit the enzymatic catalysis of phenolic compounds. The proposed electroanalytical procedures have been applied to the detection of carbamate pesticides in complex samples such as carrot, cucumber, lettuce, pepper, potato, grape, mango, orange, tangerine and lemon samples.

However, the electrostatic interactions between the FMT molecule and Lac amino acid residues remain unknown, which makes the pesticide's inhibition of Lac catalysis by phenolic compounds difficult to understand. Therefore, the development of a theoretical model to predict the interactions between FMT and amino acid residues in Lac could identify which amino acid residues are involved in the activity of FMT, with the aim of understanding the pesticide's inhibition mechanism and the sensitivity and stability of Lac-based biosensors.

Quantum mechanics (QM) has been applied successfully for systems smaller than 100 atoms, and QM can be expected to have a positive impact on the study of biological systems such as proteins that consist of a

☆ The authors declare no competing financial interest.

* Corresponding author.
E-mail address: adriana@ufc.br (A.N. Correia).

http://dx.doi.org/10.1016/j.bioelechem.2015.12.004
1567-5394/

few thousand atoms [16]. QM methods have a high computational cost, but this is offset by a more realistic modeling of the electronic nature of biological systems and the wide potential applications of QM [16]. With the development of novel computational hardware technologies in the last few decades and the development and easy access to quantum chemical software programs, QM approaches such as density functional theory (DFT) [17] can be applied to more complex systems individually or in combination with classical methods [18–20]. One approach to increase the reach of QM methods is the use of fragment-based schemes such as molecular fractionation of conjugated caps (MFCC) [21] and fragment molecular orbital (FMO) [22] methods that permit accelerated calculations in these systems without losing the calculation accuracy necessary to obtain reliable results. MFCC has been successfully applied to many systems [23–25] and involves dividing large molecules such as proteins into smaller fragments to enable the calculation of properties using a quantum mechanical approach for each fragment.

Then, the results for the individual fragments can be combined to obtain the same properties for the whole system. Using all these technological advances, we have adapted a powerful tool to improve understanding of how complex systems function and, in this specific case, of how FMT interacts with and inhibits Lac catalysis of phenolic compounds, allowing the use of this protein to fabricate electrochemical biosensors for the quantification of this pesticide in samples. Because a Protein Data Bank (PDB) file for Lac cocrystallized with FMT is not available, a docking step was necessary before the DFT calculations. The docking process predicts the best conformation of the ligand for forming a stable complex within the protein pocket [26], allowing the calculation of the interaction energy by DFT. Therefore, the aim of this investigation was to propose a quantum biochemistry calculation model to investigate the electrostatic interaction between Lac and FMT to identify which amino acid residues are responsible for the interaction and the inhibition of Lac activity, thus allowing the correlation of enzyme inhibition with the concentration of FMT in real samples.

2. Experimental section

2.1. Preparation of biosensor based in laccase enzyme and electrochemical measurements

Because the inhibition of the enzymatic catalysis process is the fundamental principle underlying the use of electrochemical biosensors for the analytical determination of pesticides in fruits and water, we fabricated an electrochemical biosensor using the Lac enzyme to evaluate the FMT pesticide inhibition of enzymatic catalysis of 4-aminophenol (4-AP, phenolic substrate) using the cyclic voltammetry technique. Following a previous published procedure,[15] the Lac enzyme (*Trametes versicolor*) was immobilized on gold electrodes previously modified with gold nanoparticles, termed here Lac/AuNPs/Au. The cyclic voltammograms were recorded with a potentiostat (Autolab PGSTAT 30, Metrohm-Eco Chemie) controlled by a personal computer, using GPES version 4.9 software. Ag/AgCl/saturated KCl, graphite rod and Lac/AuNPs/Au were used as the reference, auxiliary and working electrodes, respectively. The cyclic voltammetric (CV) experiments were performed in 0.04 mol L^{-1} of Britton–Robinson (BR) buffer pH 5.0 containing 5.83×10^{-5} mol L^{-1} of the substrate in the absence and presence of FMT pesticide and at room temperature (approximately 25 °C). The data were obtained in the range from 0.0 V to 0.4 V at 10 mV s^{-1}.

2.2. Molecular docking and system optimization

Molecular docking of FMT in the catalytic site of Lac was performed using Autodock4 [27–29]. The Lac structure was obtained from crystallographic data (PDBID 1GYC), published by [30], and the FMT ion was built and optimized through density functional theory (DFT) calculations using the Gaussian03 code [30,31]. The rm062x [32] exchange-correlation functional and the 6 − 311 + G (d,p) basis set were used, and the quality of the minimization procedure was confirmed by verifying the absence of vibrational normal modes with imaginary frequencies. FMT has a pKa of 8 [33] and, given that the biosensor measurements were obtained at pH 5, the FMT should have been charged, with an extra hydrogen atom added to the nitrogen bonded to carbon 9. The planar scheme of the FMT molecular structure and its electrostatic potential surface are presented in Fig. S1.

The charge of + 1 was then considered in the calculations. During the preparation of the input files, the atomic charge of FMT was calculated using DFT methods, and Hirshfeld's charges were assigned manually. For simplification, because Autodock is unable to assign charges for copper atoms, they were removed from the input structure of the enzyme. According to the literature [30,34], the catalytic site of Lac is in a small negatively charged cavity near copper 1, as shown in Fig. S2, which presents a cartoon view of Lac with its copper ions and highlights the binding site. During the docking of FMT, a Lamarckian genetic algorithm (GA) was used. Docking was performed 10 times using the optimized structure of FMT as the input file, a GA with 25,000,000 energy evaluations per run, the population size set to 150, and a maximum of 27,000 generations per run. At the end, five hundred poses were obtained (50 poses per output) and clustered using a RMSD tolerance of 1. $Å^2$ using Autodock Tools [29,35]. A larger cluster comprising 200 poses for FMT was generated, from which the pose with larger binding energy in the most populated cluster was chosen after a visual inspection of the interaction with the heme group. The docking results using a RMSD tolerance of 1.0 $Å^2$ can be seen in Table S1.

Next, the representative pose was complexed with Lac and submitted to energy minimization steps to improve the geometry of the binding site. The Lac–FMT complex was built using the crystallographic data for Lac and the resulting representative docking pose. Then, hydrogen atoms were added to the structure, and the water molecules and the copper atoms were replaced in the output from docking, after which the whole system was optimized by the Discovery Studio (DS) program [36]. The DS approach is based on classical molecular mechanics. During the optimization, the copper ions, FMT atoms and water molecules were kept free, and most of the protein nonhydrogen atoms were kept frozen, with the exception of residue side chains near the ligand. The CHARMm force field implemented in DS, which has specific parameters for amino acids, was used to carry out the optimization procedure. The convergence threshold parameters were set at 0.001 kcal mol^{-1} $Å^{-1}$ for the maximum force per atom, 2.0×10^{-5} kcal mol^{-1} for the total energy variation, and 1.0×10^{-5} Å for the maximum atomic displacement. The structure of the Lac–FMT complex after all treatments is shown as a cartoon in Fig. S3.

2.3. MFCC scheme and energy calculations

The classically optimized structures were then used to perform the DFT simulations, adopting the dispersion correction GGA + D exchange–correlation function, an appropriate function to describe systems with dispersive forces and hydrogen bonds, as well as van der Waals interactions. The Perdew–Burke–Ernzerhof parameterization was chosen, and it was also adopted in the scheme proposed by Tkatchenko and Scheffler (TS) to model dispersive forces [37,38]. A Double Numerical Plus Polarization (DNP 4.4) basis set was chosen to expand the Kohn–Sham orbitals within an all-electron treatment scheme. A total energy variation was imposed to be smaller than 10^{-6} Ha as a threshold to achieve self-consistency, and the orbital cutoff was set to 3.7 Å. All interaction energy calculations were performed in the gas phase (vacuum dielectric constant, ϵ^0) and were repeated with various dielectric constants, assuming values of 4, 10, 20 and 40 (ϵ^4, ϵ^{10}, ϵ^{20} and ϵ^{40}, respectively), using the COSMO continuum solvation model [39].

The Molecular Fractionation with Conjugate Caps scheme (MFCC) originally proposed by [21,40] was adopted to accomplish the description of the Lac-FMT system at the quantum level [40]. To calculate the interaction energy between the FMT with Lac residues (R^i), all amino

acid residues with at least one atom inside an imaginary surface of the FMT extending a distance of 15 Å were taken into account. The individual amino acid residue–FMT interaction energies E(FMT–R^i) were obtained by capping the residues of interest at the binding site and performing the following calculation:

$$E\left(FMT\text{–}R^i\right) = E\left(FMT\text{–}C^{-i}R^iC^i\right) - E\left(C^{-i}R^iC^i\right) - E\left(F\text{–}C^{-i}C^i\right) + E\left(C^{-i}C^i\right) \quad (1)$$

At the right side of Eq. (1), the first term, E(FMT–$C^{i-n}R^iC^{i+n}$), gives the total energy of the system formed by the FMT and the capped residue. The next term, E($C^{i-n}R^iC^{i+n}$), is the total energy of the capped residue alone, and the third term, E(FMT–$C^{i-n}C^{i+n}$), presents the total energy of the system formed by the ligand and the set of caps with hydrogen atoms placed in any broken bonds. Last, E($C^{i-n}C^{i+n}$) is the total energy of the system formed only by the hydrogenated caps. The $C^{[i]}$ cap comprises the neighboring residues R^{i-n} and R^{i+n} (n = 1, 2, 3, 4, 5) with hydrogen atoms attached to their respective broken bonds.

The binding pocket surface related to the FMT molecule was considered (BPS) with radius r as an imaginary surface centered at the FMT ion to compute the total energy of FMT binding to Lac. A binding pocket BP(r) of radius r was defined as the set of amino acid residues with at least one atom inside the corresponding BPS. Consequently, the total interaction energy for FMT complexed with Lac is a function of r and was obtained by summing all the FMT interaction energies for all BP(r) amino acid residues. The total binding energy was obtained for a 2.5–15.0 Å radius range with 0.5 Å increments.

2.4. BIRD panel and electrostatic potential surface

The interaction energies of the individual amino acid residues with FMT were plotted in a BIRD (Binding site, Interaction energy and Residues Domain) panel. In brief, the BIRD panel presents: (i) the interaction energy (in kcal mol^{-1}) of a residue, with ligand depicted using horizontal bars, from which one can quantitatively evaluate each residue relevance at the binding site, whether attractive (negative energy) or repulsive (positive energy); (ii) the most important amino acid residues contributing to the interaction, which are shown in the column of residues in the left side; (iii) the region of the FMT molecule closest to each residue; (iv) the influence of the dielectric constant, as depicted using distinct horizontal bars; and, (v) on the right side, the binding pocket radius to which each residue belongs.

To obtain the molecular electrostatic potential surfaces, the DFT electron density was projected onto a constant electron density surface. The FMT conformational structure (Fig. S1) adopted as the input for the calculation was the one presented by the molecule after docking to Lac and the atomic optimization. The total electron density was computed with a grid resolution of 0.25 Å, and the electron density isovalue was set to 0.017 electrons $Å^{-3}$ when plotting the FMT isosurface and to 0.2 electrons $Å^{-3}$ when plotting FMT with a 2.5 Å protein radius isosurface.

3. Results and discussion

Fig. 1 shows the cyclic voltammetric response of the prepared enzymatic electrode to 5.83×10^{-5} mol L^{-1} 4-aminophenol (4-AP, phenolic substrate) in the BR buffer, at pH 5.0, in the presence and absence of FMT. The voltammetric profile observed for 4-AP in the absence of pesticide is characteristic of enzymatic catalysis [41], indicating that the Lac was successfully immobilized on the gold electrode surface without loss of its biological properties. However, in the presence of FMT (dashed line), a decrease in the current densities was observed, which was associated with the interaction between the FMT molecule and amino acid residues in the Lac binding site. This result was in close agreement

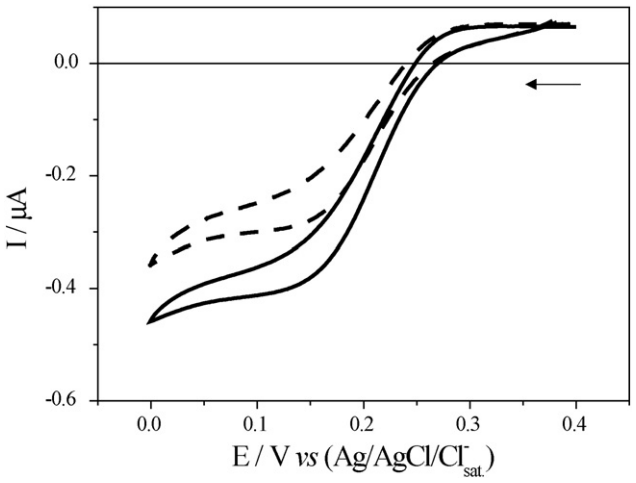

Fig. 1. Cyclic voltammograms for Lac/AuNPs/Au and 5.83×10^{-5} mol L^{-1} 4-AP in BR buffer (pH 5.0) in the absence (black line) and presence (dashed line) of FMT carbamate pesticide with a scan rate of 10 mV s^{-1}.

with results from other reports that have demonstrated that other carbamate pesticides also inhibit Lac's enzymatic activity [10–15].

Quantum calculations were performed to comprehend the inhibition of Lac by FMT. For the 155 residues within a radius of 15 Å, most of the residues exhibited FMT interaction energies with a vacuum dielectric constant (ϵ^0) of less than 10 kcal mol^{-1} in the module. Only 22 residues presented relevant energies in ϵ^0, and all of these residues were charged. The amino acid residues that demonstrated attractive interactions were Asp206, Asp456, Asp150, Glu460, Asp167, Glu302, Asp435, Asp224, Asp424 and Asp118, whereas those with repulsive interactions were Arg161, Arg121, Arg423, Arg243, Arg157, Arg22, Arg260, and Arg408. Additionally, the metallic centers (Cu1, Cu2, Cu3 and Cu4) in the enzyme site also formed repulsive interactions to FMT. However, most of these residues lost their relevance as soon as the dielectric constant was considered and increased, and noncharged residues were found to be relevant.

The results, in terms of the vacuum dielectric constant (ϵ^0), of the FMT interaction energies with some of the important Lac residues within 8.5 Å were as follows: −84.34 kcal mol^{-1} (Asp206), −47.55 kcal mol^{-1} (Asp456), −45.17 kcal mol^{-1} (Asp150), −42.07 kcal mol^{-1} (Glu460), −7.69 kcal mol^{-1} (Cys453), −7.59 kcal mol^{-1} (Pro207), −6.93 kcal mol^{-1} (Ile455), −6.30 kcal mol^{-1} (Gly392) and 76.23 kcal mol^{-1} (Cu4). The energies obtained considering the solvation model are very different from the ones obtained for ϵ^0. For example, adopting ϵ^4, the interaction energy values for the same residues are as follows: −32.84 kcal mol^{-1} (Asp206), −−13.49 kcal mol^{-1} (Asp456), −14.00 kcal mol^{-1} (Asp150), −12.40 kcal mol^{-1} (Glu460), −6.01 kcal mol^{-1} (Cys453), −4.40 kcal mol^{-1} (Pro207), −4.29 kcal mol^{-1} (Ile455), −4.07 kcal mol^{-1} (Gly392) and 24.50 kcal mol^{-1} (Cu4). The dielectric constant has a great influence on the interaction energy of the ligand with the enzyme residues, but mainly influences the interaction energy values of the charged residues, even if those residues are distant from the ligand. The most important interaction energies between FMT and the Lac residues are presented in the BIRD panel (Fig. 2) for all of the dielectric constants ϵ^0, ϵ^4, ϵ^{10}, ϵ^{20} and ϵ^{40}, according to the proximity to the regions of the molecule (in the left of the panel) and the distance (the black numbers in the right of the panel). The interaction energies with the FMT obtained for all the 155 residues present the interaction radius of 15 Å are shown in the Tables S2, S3 and S4 in the Supporting Information.

In addition, the dielectric constant influenced the most of the residue–FMT interaction energies, especially those related to charged residues such as Arg161 and Asp456. For instance, the energies varied

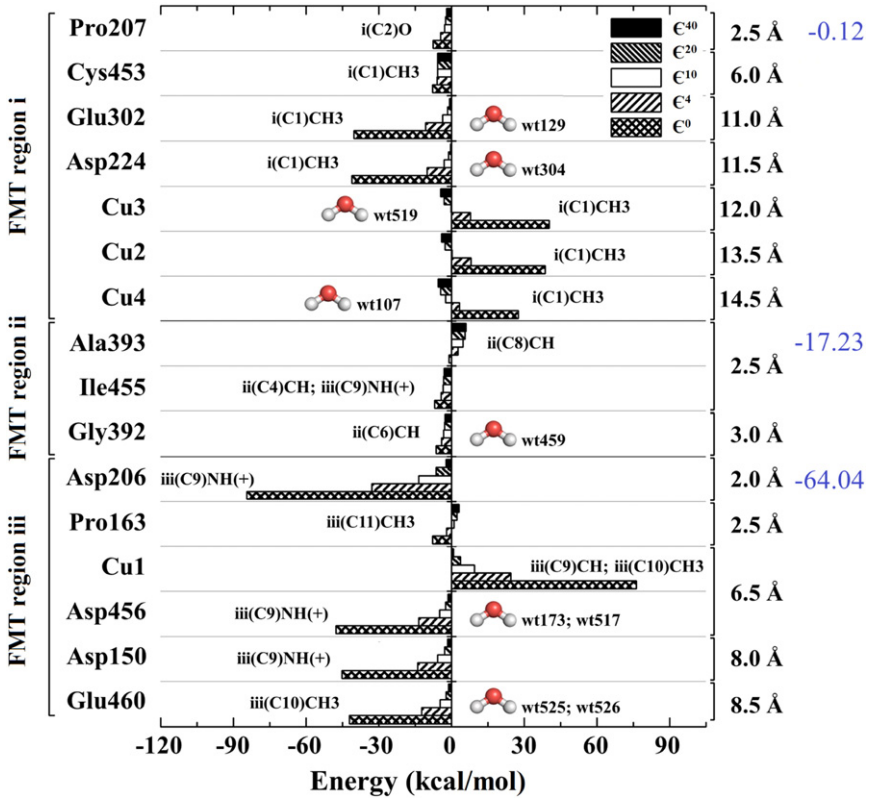

Fig. 2. Interaction energies from the BIRD panel for the dielectric constants 0, 4, 10, 20 and 40 with the most relevant residues, divided according to the proximity of the regions to the FMT molecule.

from 29.15 kcal mol^{-1} and −47.55 kcal mol^{-1} at ϵ^0 to −4.45 kcal mol^{-1} and −4.98 kcal mol^{-1} at ϵ^{10} for Arg161 and Asp456, respectively and from 4.45 kcal mol^{-1} at ϵ^0 (Arg161) and −4.98 kcal mol^{-1} at ϵ^{10} (Asp456) to 1.58 kcal mol^{-1} and −1.36 kcal mol^{-1} (Arg161 and Asp456, respectively) when the dielectric constant was ϵ^{40}. The variation in the energies was also observed to a lesser degree for noncharged residues such as Pro207, which exhibited energies −7.59 kcal mol^{-1}, −2.95 kcal mol^{-1} and −2.13 kcal mol^{-1} at the dielectric constants ϵ^0, ϵ^{10} and ϵ^{40}, respectively.

Considering the interaction energies in a vacuum and at the dielectric constants of ϵ^4, ϵ^{10} and ϵ^{20}, the most relevant residue was found to be Asp206. Another interesting point was that the dielectric constant did not affect the interaction energy between FMT and Cys453, possibly indicating some relevance of this residue to the Lac–FMT interaction. Cys453 is 5.78 Å away from the ligand, and its interaction energy was not large when compared to that of other amino acids if considered at low dielectric constants (ϵ^0 and ϵ^4). However, this residue's energy became relevant when the dielectric constants ϵ^{10}, ϵ^{20} and ϵ^{40} were considered. Lac is a metalloprotein containing four copper ions (Cu^{2+}): Cu1, Cu2, Cu3 and Cu4. These cations should interfere somewhat negatively with the Lac-FMT interaction because FMT is also a cation with a +1 charge at pH 5. All of the interaction energies between Cu^{2+} and FMT at ϵ^0 are positive, indicating a repulsion interaction. The closer the Cu^{2+} to FMT, the stronger the repulsion observed (in order of proximity to FMT: 76.23 kcal mol^{-1}, 40.21 kcal mol^{-1}, 38.60 kcal mol^{-1} and 27.49 kcal mol^{-1} for Cu1, Cu3, Cu2 and Cu4, respectively).

In the BIRD panel in Fig. 2, the distribution of the water molecules in relation to the residues, as well the total interaction energy, is shown for all of the residues within a 15 Å radius, according to their proximity to each part of the FMT molecule at ϵ^4 (blue numbers in the right side of BIRD panel in Fig. 2). This piece of information reveals that the most relevant protein residues are closer to the charged part of FMT, which is region iii (see Fig. S1).

The relative distribution of some of the most relevant residues in relation to the FMT molecule is presented in Scheme 1 in two different views. In Scheme 1B, a hydrogen bond can be clearly seen between the ammonium of the FMT and the oxygen from the carboxylic group of Asp206, which reinforces the relevance of this residue to the stability of the Lac–FMT interaction. The other residue with which the FMT forms a hydrogen bond is Asn208, but their interaction energy is not significant (see Supporting Information).

Additionally, the contribution of each 0.5 Å ligand shell (considering the FMT surface) to the total interaction energy of the 15 Å radius was computed and is presented in Fig. 3. The smallest shell was 2 Å, and the largest was 15 Å. The two first shells with 2 Å and 2.5 Å are strongly attractive. The next 4 layers presented little or no contribution. Then, the 5 Å shell was repulsive, and was followed by another two layers with very little contribution. The 6.5 Å layer was another quite repulsive shell, and it was followed again by two more low contribution shells. The 8 Å and 8.5 Å layers generated attractive contributions, and the next three layers were not highly relevant. Then, the shells 10.5 Å, 11 Å and 11.5 Å were all relevant, with the first being repulsive and the other two attractive. The next the three layers were not highly important, and the last four shells (13.3 Å, 14 Å, 14.5 Å and 15 Å) were relevant and repulsive. However, as the dielectric constant increased, the relevance of the further shells decreased. The shells were divided into three groups: close residues (shells 2 Å through 6 Å), intermediate residues (6.5 Å to 10.5 Å) and distant residues (11 Å to 15 Å).

Scheme 2 shows how the residues are divided between the three groups and displayed around the FMT. The group with the largest contribution is that of the close residues, −146.72 kcal mol^{-1} at ϵ^0. The other two groups have contributions at ϵ^0 of −37.05 kcal mol^1 and 7.39 kcal mol^{-1} (intermediate and distant residue groups, respectively).

The Lac–FMT system's total interaction energy as a function of the radius of interaction is presented in Fig. 4, which takes into consideration the energy of all 155 residues present in a 15 Å radius.

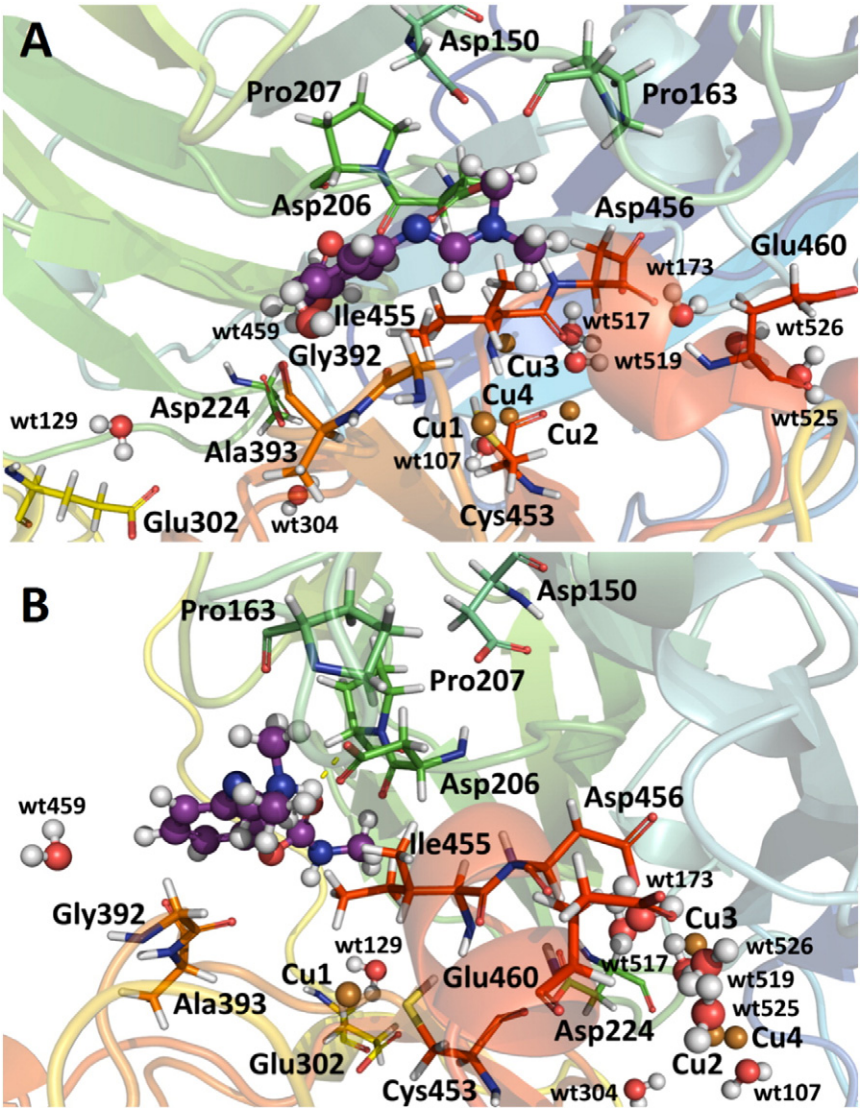

Scheme 1. Schematic representation of the binding pocket of the Lac showing the most important residues involved in the binding interaction in two different views. The only relevant residue that forms a hydrogen bond with FMT is Asp206, as shown in B.

The relevant residues are highlighted according to the radius of interaction to which they belong and the dielectric constant at which they remain relevant in Fig. 4. The smallest radius with residues (2 Å) presented a ϵ^0 interaction energy of −84.34 kcal mol^{-1}, which decreased to −32.84 kcal mol^{-1}, −13.62 kcal mol^{-1}, −6.31 kcal mol^{-1} and −2.31 kcal mol^{-1} at ϵ^4, ϵ^{10}, ϵ^{20} and ϵ^{40}, respectively. With an

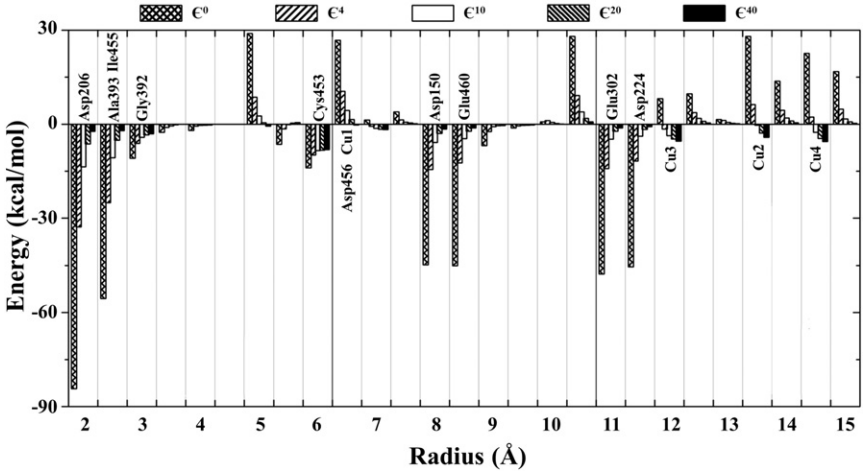

Fig. 3. Contribution of each 0.5 Å amino acid residue surface shell to the total interaction energy.

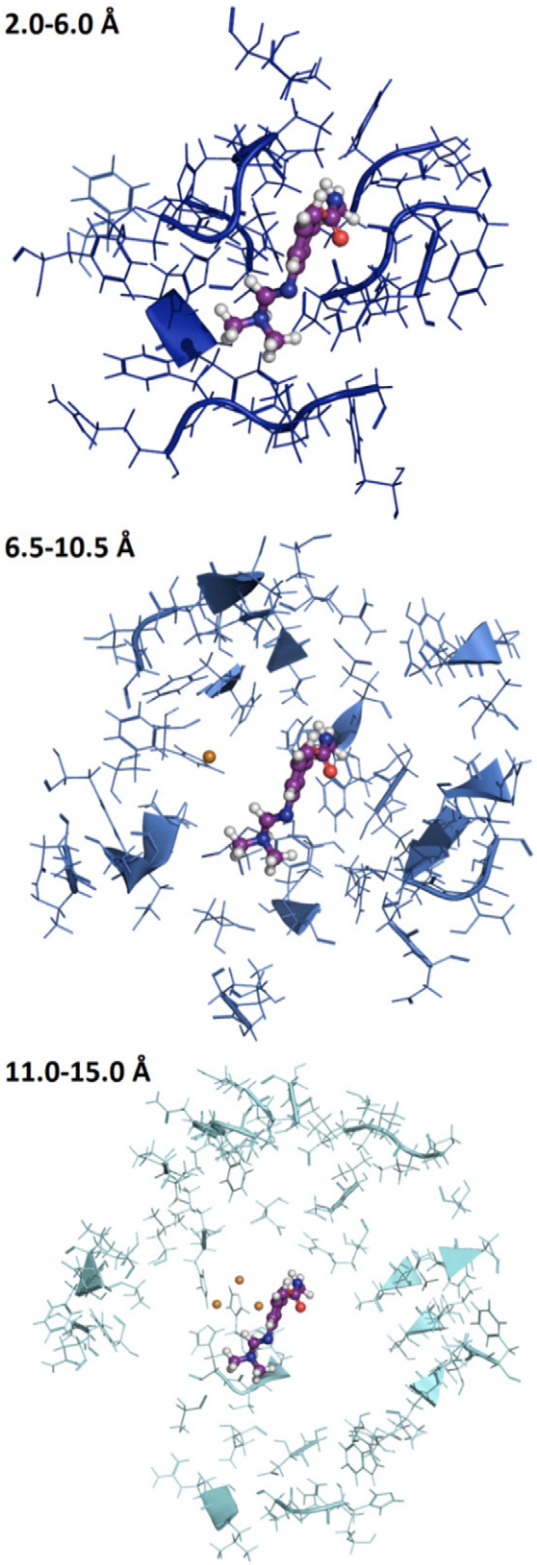

Scheme 2. Schematic representation of the cartoon view of the three groups of residues. Top: residues present in the shells from 2 Å to 6 Å (dark blue). Middle: residues present in the layers 6.5 Å to 10.5 Å (blue). Bottom: residues of the shells present at a distance of 11 Å to 15 Å (light blue).

increase in the binding site radius to 3 Å, the addition of more residues decreased the total interaction energy for all of the dielectric constants, indicating the presence of more attractive residues. The total interaction energy curve for the system in vacuum (ϵ^0) clearly indicates the

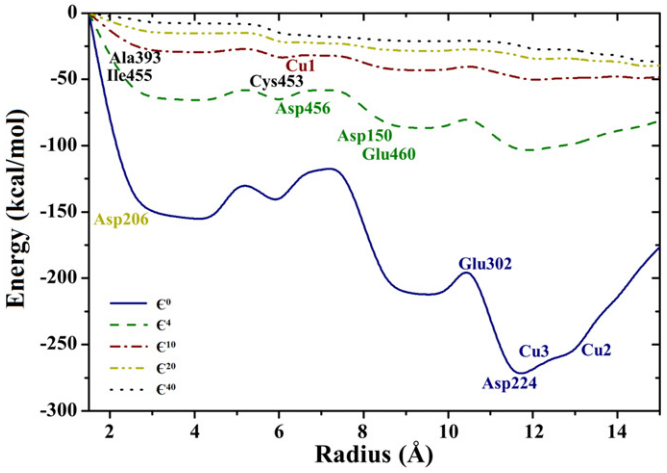

Fig. 4. Total interaction energy for Lac–FMT as a function of the binding pocket surface radius for the dielectric constants ϵ^0, ϵ^4, ϵ^{10}, ϵ^{20} and ϵ^{40}.

existence of a radius with attractive residues and a radius with repulsive residues. This result was observed because, for the ϵ^0, even distant residues present high interaction energies if they are charged. According to the curve for ϵ^0, an attractive region for Lac–FMT interactions is formed within a radius of 4.5 Å, corroborating the literature supposition that close residues stabilize the radical cation products from the catalytic cycle [30]. Also, in the curve for ϵ^0, four regions with repulsive residues can be clearly observed: at a radius of 5 Å (Arg161), 6.5 Å (Cu4) and 10.5 Å (Arg121 and Arg423), and most radii after 12.5 Å (12.5 Å — Arg157; 13.5 Å — Arg22 and Cu2; 14 Å — Arg260; 14.5 Å — Cu3; 15 Å — Arg408). Succeeding the radii 5 Å, 6.5 Å and 10 Å are radii with attractive residues: Cys453 (6 Å), Asp150 (8 Å), Glu460 (8.5 Å), Glu302 and Asp435 (11 Å), and Asp224 (11.5 Å). As the dielectric constant is considered and increased, the radii exhibiting repulsion start to become less relevant or to even disappear. Also, the distant attractive radii exhibit less relevance. This change is a reflection of the decrease in the interaction energy between the charged residues and the FMT and also highlights the importance of the dielectric constant when studying the interaction energies for Lac–FMT.

The electrostatic potential projected onto the electron density isosurface for FMT and the residues within a 2.5 Å radius is presented in Scheme 3. The attraction between the carboxylic group of Asp206 and the ammonium group of FMT can be clearly observed through the difference in the electrostatic potential of these groups, confirming the residue's relevance to the stability of the Lac–FMT interaction.

4. Conclusions

The electrochemical measurements indicated that Lac's enzymatic catalysis of phenol compounds was inhibited by the pesticide FMT. The quantum chemical calculations based on DFT with a protein fragmentation approach were successfully used to elucidate how the FMT molecule inhibits Lac and to identify the most relevant amino acid residues that interact with FMT in the enzyme's binding domain. Asp206 was the residue which demonstrated great relevance to the pesticide's binding. The residue Cys453 also appeared to be important, because the Cys453–FMT interaction energy was not affected by the dielectric constant, although it is not a very close residue.

Acknowledgments

The authors wish to thank the Brazilian agencies CNPq (400223/2014-7), CAPES (313/11) and FINEP (22001018034P4) for their financial support. The calculations were partially performed at CENAPAD — UFC.

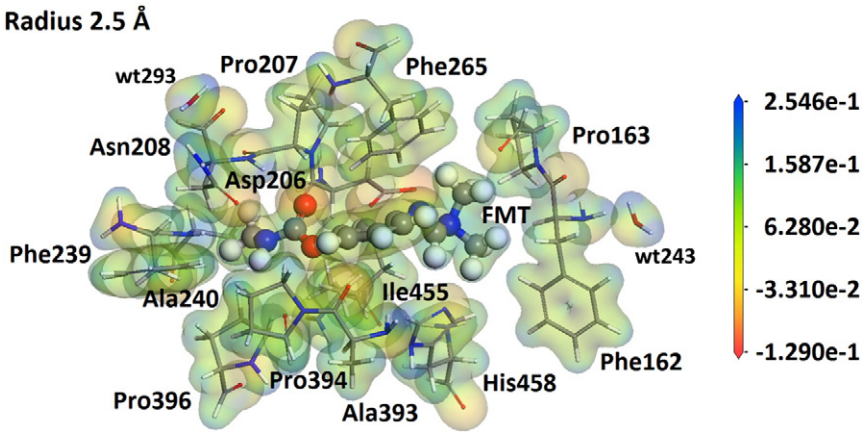

Scheme 3. Schematic representation of the projection of the electrostatic potential onto the electron density isosurface of FMT and the ligand binding domain residues within a radius of 2.5 Å.

Appendix A. Supplementary data

Computational details. Fig. S1 shows the FMT structure divided into three regions according to the characteristics of each region and considering the electrostatic potential surface results for FMT. Fig. S2 shows a cartoon representation of Lac with copper ions. Fig. S3 shows a cartoon representation of the Lac—FMT complex. Table S1 shows the docking results. Tables S2, S3 and S4 show the MFCC results. Supplementary data associated with this article can be found in the online version, at doi:http://dx.doi.org/10.1016/j.bioelechem.2015.12.004.

References

[1] H.S. Rathore, L.M.L. Nollet, Pesticides: Evaluation of Environmental, CRC, New York, USA, 2012.
[2] S.D. Richardson, T.A. Ternes, Water analysis: emerging contaminants and current issues, Anal. Chem. 86 (2014) 2813–2848.
[3] United States Environmental Protection Agency. http://www.epa.gov/opptintr/aegl/pubs/priority_2.htm. (Accesed Feb 14, 2015).
[4] J.S.V. Dyk, B. Pletschke, Review on the use of enzymes for the detection of organochlorine, organophosphate and carbamate pesticides in the environment, Chemosphere 82 (2011) 291–307.
[5] K. Fenner, S. Canonica, L.P. Wackett, M. Elsner, Evaluating pesticide degradation in the environment: blind spots and emerging opportunities, Science 341 (2013) 752–758.
[6] S. Padilla, R.S. Marshall, D.L. Hunter, A. Lowit, Time course of cholinesterase inhibition in adult rats treated acutely with carbaryl, carbofuran, formetanate, methomyl, methiocarb, oxamyl or propoxur, Toxicol. Appl. Pharmacol. 219 (2007) 202–209.
[7] C.B. Divito, S. Davies, S. Masoudi, C.N. Muhoro, Relative stability of formamidine and carbamate groups in the bifunctional pesticide formetanate hydrochloride, J. Agric. Food Chem. 55 (2007) 5377–5382.
[8] D.P. Nikoleles, T. Varzakas, A. Erdem, G. Nikoleli, Portable Biosensing of Food Toxicants and Environmental Pollutants, CRC, New York, USA, 2013.
[9] M. Govindhan, B. Adhikari, A. Chen, Nanomaterials–based electrochemical detection of chemical contaminants, RSC adv. 4 (2014) 63741–63760.
[10] S.F. Fernandes, I.C. Vieira, A.M.J. Barbosa, V.S. Ferreira, Methomyl detection by inhibition of laccase using a carbon ceramic biosensor, Electroanalysis 23 (2011) 1623–1630.
[11] T.M.B.F. Oliveira, M.F. Barroso, S. Morais, P. De Lima-Neto, A.N. Correia, M.B.P.P. Oliveira, C. Delerue-Matos, Biosensor based on multi-walled carbon nanotubes paste electrode modified with laccase for pirimicarb pesticide quantification, Talanta 106 (2013) 137–143.
[12] E. Zapp, D. Brondani, I.C. Vieira, C.W. Scheeren, J. Dupont, A.M.J. Barbosa, V.S. Ferreira, Biomonitoring of methomyl pesticide by laccase inhibition on sensor containing platinum nanoparticles in ionic liquid phase supported in montmorillonite, Sensors Actuators B Chem. 155 (2011) 331–339.
[13] T.M.B.F. Oliveira, M.F. Barroso, S. Morais, M. Araújo, C. Freire, A.N. Correia, P. De Lima-Neto, M.B.P.P. Oliveira, C. Delerue-Matos, Laccase—Prussian blue film-graphene doped carbon paste modified electrode for carbamate pesticides quantification, Biosens. Bioelectron. 47 (2013) 292–299.
[14] T.M.B.F. Oliveira, M.F. Barroso, S. Morais, M. Araújo, C. Freire, A.N. Correia, P. De Lima-Neto, M.B.P.P. Oliveira, C. Delerue-Matos, Sensitive bi-enzymatic biosensor based on polyphenoloxidases-gold nanoparticles-chitosan hybrid film-graphene doped carbon paste electrode for carbamates detection, Bioelectrochemistry 98 (2014) 20–29.
[15] F.W.P. Ribeiro, M.F. Barroso, S. Morais, S. Viswanathan, P. De Lima-Neto, A.N. Correia, M.B.P.P. Oliveira, C. Delerue-Matos, Simple laccase-based biosensor for formetanate hydrochloride quantification in fruits, Bioelectrochemistry 95 (2014) 7–14.
[16] K.M. Merz Jr., Using quantum mechanical approaches to study biological systems, Acc. Chem. Res. 47 (2014) 2804–2811.
[17] P. Hohenberg, W. Kohn, Inhomogeneous electron gas, Phys. Rev. 136 (1964) B864–B871.
[18] D. Mucs, R.A. Bryce, The application of quantum mechanics in structure-based drug design, Expert Opin. Drug Discov. 8 (2013) 263–276.
[19] J. Hafner, A joint effort with lasting impact, Nat. Mater. 9 (2010) 690–692.
[20] W.L. Jorgensen, The many roles of computation in drug discovery, Science 303 (2004) 1813–1818.
[21] X. Wang, J. Liu, J.Z.H. Zhang, X. He, Electrostatically Embedded Generalized Molecular Fractionation with Conjugate Caps Method for Full Quantum Mechanical Calculation of Protein Energy, J. Phys. Chem. A 117 (2013) 7149–7161.
[22] D.G. Fedorov, T. Nagata, K. Kitaura, Exploring chemistry with the fragment molecular orbital method, Phys. Chem. Chem. Phys. 14 (2012) 7562–7577.
[23] R.F. Costa, V.N. Freire, E.M. Bezerra, B.S. Cavada, E.W.S. Caetano, Explaining statin inhibition effectiveness of HMG—CoA reductase by quantum biochemistry computations, Phys. Chem. Chem. Phys. 14 (2012) 1389–1398.
[24] C.R.F. Rodrigues, J.I.N. Oliveira, U.L. Fulco, E.L. Albuquerque, R.M. Moura, E.W.S. Caetano, V.N. Freire, Quantum biochemistry study of the T3—785 tropocollagen triple-helical structure, Chem. Phys. Lett. 559 (2013) 88–93.
[25] I.L. Barroso-Neto, J.P.C. Marques, R.F. Costa, E.W.S. Caetano, B.S. Cavada, C. Gottfried, V.N. Freire, Inactivation of ovine cyclooxygenase-1 by bromoaspirin and aspirin: a quantum chemistry description, J. Phys. Chem. B 116 (2012) 3270–3279.
[26] R.T. Kroemer, Structure-based drug design: docking and scoring, Curr. Protein Pept. Sci. 8 (2007) 312–328.
[27] G.M. Morris, D.S. Goodsell, R.S. Halliday, R. Huey, W.E. Hart, R.K. Belew, A.J. Olson, Automated docking using a Lamarckian genetic algorithm and an empirical binding free energy function, J. Comput. Chem. 19 (1998) 1639–1662.
[28] R. Huey, G.M. Morris, A.J. Olson, D.S. Goodsell, A semiempirical free energy force field with charge-based desolvation, J. Comput. Chem. 28 (2007) 1145–1152.
[29] G.M. Morris, R. Huey, W. Lindstrom, M.F. Sanner, R.K. Belew, D.S. Goodsell, A.J. Olson, AutoDock4 and AutoDockTools4: automated docking with selective receptor flexibility, J. Comput. Chem. 30 (2009) 2785–2791.
[30] K. Piontek, M. Antorini, T. Choinowski, Crystal structure of a laccase from the fungus *Trametes versicolor* at 1.90—a resolution containing a full complement of coppers, J. Biol. Chem. 270 (2002) 37663–37669.
[31] M.J. Frisch, G.W. Trucks, H.B. Schlegel, G.E. Scuseria, M.A. Robb, J.R. Cheeseman, G. Scalmani, V. Barone, B. Mennucci, G.A. Petersson, et al., Gaussian 09, Revision A.01, Gaussian, Inc., Wallingford, CT, USA, 2009.
[32] Y. Zhao, D.G. Truhlar, The M06 suite of density functionals for main group thermochemistry, thermochemical kinetics, noncovalent interactions, excited states, and transition elements: two new functionals and systematic testing of four M06-class functionals and 12 other functionals, Theor. Chem. Accounts 120 (2008) 215–241.
[33] Conclusion regarding the peer review of the pesticide risk assessment of the active substance formetanate, EFSA Sci. Rep. 69 (2006) 1–78.
[34] T. Bertrand, C. Jolivalt, P. Briozzo, E. Caminade, N. Joly, C. Madzak, C. Mougin, Crystal structure of a four—copper laccase complexed with an arylamine: insights into substrate recognition and correlation with kinetics, Biochemistry 41 (2002) 7325–7333.
[35] M.F. Sanner, Python: a programming language for software integration and development, J. Mol. Graph. Model. 17 (1999) 57–61.
[36] Dassault Systèmes BIOVIA, Discovery Studio Modeling Environment, Release 3.1, San Diego, 2011.
[37] J.P. Perdew, K. Burke, M. Ernzerhof, Generalized gradient approximation made simple, Phys. Rev. Lett. 77 (1996) 3865–3868.

[38] A. Tkatchenko, M. Scheffler, Accurate molecular Van Der Waals interactions from ground-state electron density and free-atom reference data, Phys. Rev. Lett. 102 (2009) 1–4.
[39] A. Klamt, G. Schüürmann, COSMO: a new approach to dielectric screening in solvents with explicit expressions for the screening energy and its gradient, J. Chem. Soc. Perkin Trans. 2 (1993) 799–805.
[40] D. Zhang, J. Zhang, Molecular fractionation with conjugate caps for full quantum mechanical calculation of protein–molecule interaction energy, J. Chem. Phys. 119 (2003) 3599–3605.
[41] C. Tortoline, M.D. Fusco, M. Frasconi, G. Favero, F. Mazzei, Laccase — polyazetidine prepolymer–MWCNT integrated system: biochemical properties and application to analytical determination in real samples, Microchem. J. 96 (2010) 301–307.